

## OBSERVABLES IN THE 3 FLAVOR PNJL MODEL AND THEIR RELATION TO EIGHT QUARK INTERACTIONS\* \*\*

B. HILLER, J. MOREIRA, A.A. OSIPOV, A.H. BLIN

Departamento de Física, CFC  
Faculdade de Ciências e Tecnologia da Universidade de Coimbra  
3004-516 Coimbra, Portugal

*(Received September 4, 2012)*

Several relevant thermodynamic observables obtained within the (2+1) flavor and spin zero NJL and PNJL models with inclusion of the 't Hooft determinant and  $8q$  interactions are compared with lattice-QCD (lQCD) results. In the case that a small ratio  $R = \frac{\mu_B}{T_c} \sim 3$  at the critical end point (CEP) associated with the hadron gas to quark-gluon plasma transition is considered, combined with fits to the lQCD data of the trace anomaly, subtracted light quark condensate and continuum extrapolated data of the light quark chiral condensate, a reasonable description for the PNJL model is obtained with a strength  $g_1 \sim 5 \dots 6 \times 10^3 \text{ GeV}^{-8}$  of the  $8q$  interactions. The dependence on the further model parameters is discussed.

DOI:10.5506/APhysPolBSupp.5.1171

PACS numbers: 11.10.Wx, 11.30.Rd, 11.30.Qc

In recent years, the role of effective chiral Lagrangians has grown as an important indicator of the order and universality class of phase transitions, as well as of the nature and location of the related CEP that may occur for the ground state of QCD in presence of external parameters, such as finite temperature  $T$ , baryonic chemical potential  $\mu_B$ , magnetic field  $B$  [1]. In parallel, lQCD advances at zero and moderate chemical potential with masses approaching the physical values of the light quarks [2] and pion

---

\* Presented by B. Hiller at the Workshop "Excited QCD 2012", Peniche, Portugal, May 6–12, 2012.

\*\* Work supported by FCT, CERN/FP/116334/2010, QREN, UE/FEDER through COMPETE. Part of the EU Research Infrastructure Integrating Activity Study of Strongly Interacting Matter (HadronPhysics3) under the 7th Framework Programme of EU: Grant Agreement No. 283286.

mass [3], strongly indicate at a crossover transition from the hadronic to the quark-gluon phase at finite  $T$  and  $\mu_B = 0$ . Combining IQCD and chemical freeze-out data from relativistic heavy-ion collision facilities, the location of the CEP is presently conjectured to eventually occur at  $R = \frac{\mu_B}{T_c} \sim 2$  and  $\frac{T}{T_c} \sim 1$ , [4, 5].

We consider the SU(3) flavor and spin-0 Nambu–Jona-Lasinio model (NJL) [6] with inclusion of the U(1)<sub>A</sub> breaking 't Hooft flavor determinant [7–9] and eight quark ( $8q$ ) interactions [10, 11] (of which there exist two types, one of them violating the OZI rule, with strength  $g_1$ ), and extend it to include the Polyakov loop (PNJL) [12–21]. The  $8q$  have been firstly introduced to stabilize the effective potential of the model [10]. Their role turned out to be of significant importance in the behavior of model observables in presence of external parameters [17–19, 22–25]. Of particular interest is that the  $8q$  coupling strengths  $g_1$  can be varied in tune with the  $4q$  interaction strength  $G$  without changing the vacuum condensates and low energy meson spectra, except for the  $\sigma$ -meson mass  $m_\sigma$  which decreases with increasing  $g_1$ . Fits to the low lying pseudoscalar and scalar meson spectra yield  $m_\sigma \sim 560$  MeV for  $g_1 = 6000$  GeV<sup>-8</sup> and  $m_\sigma \sim 690$  MeV for  $g_1 = 1500$  GeV<sup>-8</sup> [11]. In the  $\mu, T$  plane (where  $\mu = \frac{\mu_B}{3}$ ), the  $g_1, G$  interplay gives rise to a line of CEP, starting from the regime of large ratios  $R \sim 20$  (NJL) and  $R \sim 10$  (PNJL) in the case of weak  $8q$  coupling  $g_1$ , to small ratios for strong  $g_1$ . In the first case, the chiral condensate is related with spontaneous symmetry breaking (SSB) driven by  $4q$  interactions, in the second scenario SSB is induced by the  $6q$  't Hooft strength [11, 23, 25]. This continuous set of CEP is particular to the  $8q$  extension of the model. However, a correlation between  $m_\sigma$  and the location of the CEP is also observed in the (2+1)-flavor quark-meson Lagrangian, where besides the 't Hooft term, a quartic mesonic contribution is present [26, 27], thus bearing a resemblance to the semi-bosonized version of the  $8q$  NJL Lagrangian [11]. In order to restrict the  $g_1$  values, one may: (i) calculate decays and scattering in the vacuum which are expected to narrow the choice, and (ii) compare with available IQCD data at finite  $T$  and moderate  $\mu$ . In the present study, we try to explore the second option. For the PNJL case an extra uncertainty arises due to the parameters related with the choice of Polyakov potential  $\mathcal{U}_P$ . In particular, the  $T_0$  parameter of [14, 15] has a sizeable effect on the transition temperature.

First, we show in Fig. 1 the CEP lines in a  $(\mu, T)$  versus  $g_1$  diagram. The PNJL model (solid lines) enhances the effect of pushing  $R$  to small values as functions of  $g_1$  in comparison with the NJL case (dashed lines). The crossing of the CEP( $T$ ) and CEP( $\mu$ ) lines, (yielding  $R = 3$ ), is reached for the PNJL at  $g_1 \sim 6.4 \times 10^3$  GeV<sup>-8</sup>, for the choice  $T_0 = 190$  MeV, whereas it occurs for the NJL only at a much larger value,  $g_1 \sim 8.4 \times 10^3$  GeV<sup>-8</sup> (we remind that

with increasing  $g_1$  the crossover becomes sharper and eventually gives rise to a first order transition at  $\mu = 0$ , which happens at  $g_1 \sim 9 \times 10^3 \text{ GeV}^{-8}$  in the NJL case). Changing  $T_0$ , the CEP( $T$ ) is shifted up (down) with increasing (decreasing)  $T_0$  (see caption of Fig. 1), while CEP( $\mu$ ) remains sensibly unaltered.

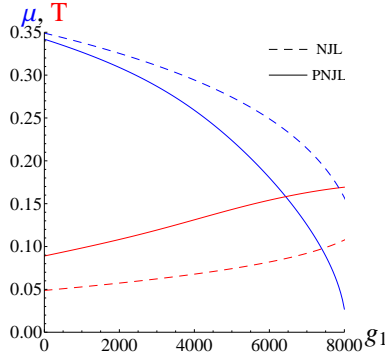


Fig. 1. Pairs  $(T, \mu)$  of CEP as function of the  $8q$  interaction strength  $g_1$ . Positive slope lines (red online) show  $T$ -dependence, negative slope lines (blue online) show  $\mu$  dependence. All model parameters fixed as in [25], except for  $g_1, G$ . PNJL potential from [14]. Intersection ( $R = 3$ ) of PNJL curves (solid lines) occur at  $(\mu = T = 158; 167; 188 \text{ MeV})$  with  $g_1 = 6436; 6251; 6127 \text{ GeV}^{-8}$  for  $T_0 = 190; 210; 270$  respectively (shown only for  $T_0 = 190 \text{ MeV}$ ). Intersection of NJL curves (dashed lines) at  $\mu = T = 117$  with  $g_1 = 8372 \text{ GeV}^{-8}$ .

In Fig. 2, the chiral condensates and dressed Polyakov loop for  $u, s$  quarks are shown for the NJL as function of  $T$  for  $\mu = 0$  and with varying strength  $g_1$  (see caption). For  $g_1 10^{-3} = 1; 5; 6.5; 8 \text{ GeV}^{-8}$  the transition temperatures  $T_t$  defined at the corresponding inflection points of the curves are  $T_t = 192; 163; 147; 135 \text{ MeV}$  for the  $u$ -condensate,  $T_t = 197; 163; 150; 135 \text{ MeV}$  for the  $u$ -quark dressed Polyakov loop,  $T_t = 197; 160; 147; 135 \text{ MeV}$  at the first inflection point of  $s$ -quark condensate,  $T_t = 270; 240; 235; 225 \text{ MeV}$  at its 2nd inflection point,  $T_t = -; 166; 150; 135 \text{ MeV}$  at 1st inflection point of the dressed  $s$ -quark Polyakov loop and  $T_t = 270; 240; 235; 225 \text{ MeV}$  at its 2nd inflection point. The 1st set of inflection points in the case of the  $s$ -quark condensate and dressed Polyakov loop occur due to the gap equations that correlate the  $u$  and  $s$  variables, yielding similar  $T_t$  for the  $u$  and  $s$  observables. The 2nd inflection point occurs at temperatures  $T_t$  larger by  $\sim 80 \text{ MeV}$ .

A similar pattern is observed for the PNJL model in Fig. 3, the second inflection points occur at roughly  $55 \text{ MeV}$  higher  $T_t$  values. Visually, these 2nd inflection points can barely be detected, the transition is very slow and smooth. This behavior can be traced back to the fact that for large  $T$  the

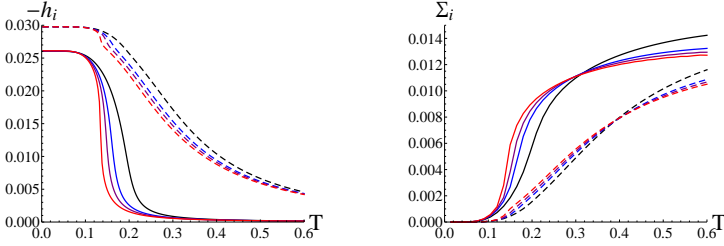


Fig. 2. The chiral condensates  $= h_i/2$ ,  $i = u, s$  and the dressed Polyakov loop  $\Sigma^i$  as functions of  $T$  for NJL; solid lines for light quarks, dashed for the strange quark. Up to down curves in left panel:  $g_1 \times 10^{-3} = 1; 5; 6.5; 8 \text{ GeV}^{-8}$ , corresponding to black, blue, violet, red (color online). Same ordering in right panel, after crossing point.

$s$ -quark constituent quark mass approaches asymptotically its current quark mass value, which is much larger than for the  $u$ -quark<sup>1</sup>. It is a disputable matter which temperature should be taken to characterize the transition for the  $s$ -quark in these observables. A calculation of the chiral and quark number susceptibilities associated with the  $s$ -quark in the NJL model display only one peak characterizing the transition temperature.

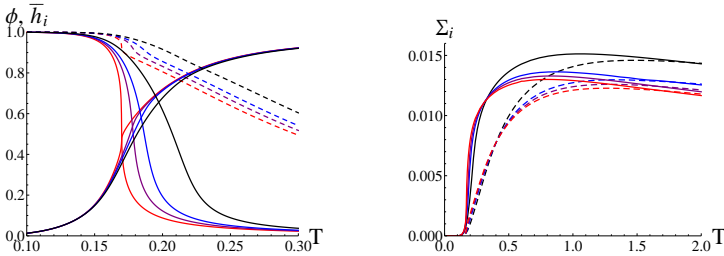


Fig. 3. The same as in Fig. 1 for the PNJL model. In left panel  $\phi$  (curves growing with  $T$ ) stand for the Polyakov loop and corresponding  $g_1$  strengths revert order compared to the chiral condensate.

In Fig. 4, one sees however that in the PNJL case two peaks can occur again for the  $s$ -quark chiral susceptibility. Fig. 5 (left) shows the trace anomaly calculated for  $g_1 = 6000 \text{ GeV}^{-8}$ , for various values of the parameter  $T_0$  in comparison with lattice data. In Fig. 5 (right), the subtracted condensate  $\Delta_{ls}$  is shown for several values for  $g_1$ , calculated with  $T_0 = .19 \text{ GeV}$ , and compared to lQCD. In Fig. 6, the light chiral condensate is compared with lQCD data extrapolated to the continuum limit [2] for different values of  $g_1$  and with  $\mathcal{U}^1$  for the cases  $T_0 = .15 \text{ GeV}$  (left) and  $T_0 = .19 \text{ GeV}$  (right).

<sup>1</sup> We calculate the thermodynamic potential with the prescription of [21, 25], where we show that it leads to the correct large  $T$  asymptotic behavior for the quark masses (condensates), traced Polyakov loop and number of degrees of freedom.

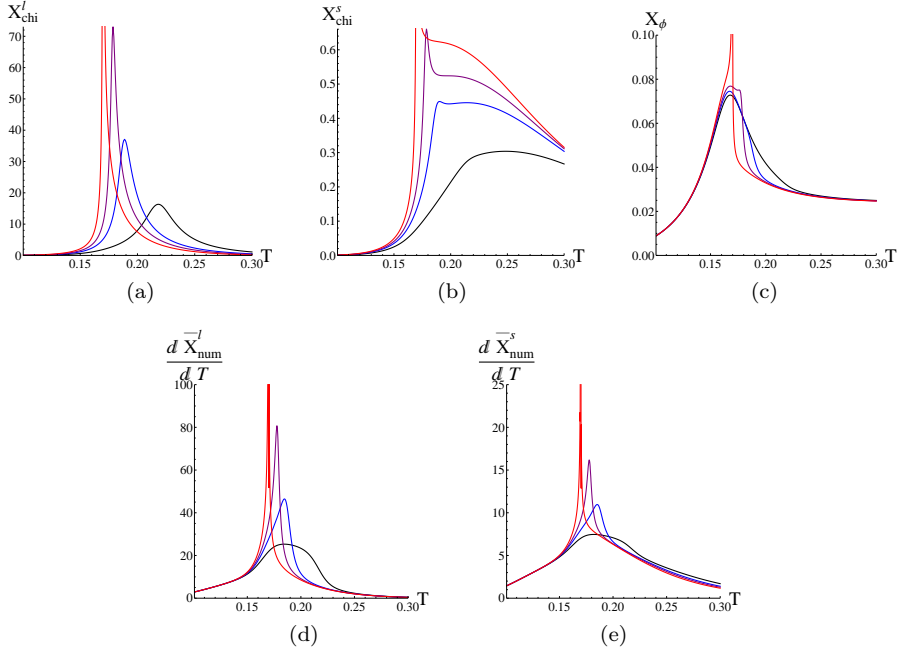


Fig. 4. Susceptibilities for PNJL,  $\mathcal{U}_P$  of [14] and  $T_0 = 190$  MeV. (a) light quark chiral susceptibilities, (b)  $s$  quark chiral susceptibilities, (c) Polyakov loop susceptibility, (d) quark number (for  $u$  quark) and (e) quark number (for  $s$ -quark) susceptibilities. The peaks get more pronounced with increasing  $g_1$ . Color code as in Fig. 2.

From these comparisons we conclude (i) that the smaller the ratio  $R = \frac{\mu_B}{T_c}$  related with the CEP location, the larger the  $8q$  interaction strength  $g_1$  must be chosen; a sizeable dependence on the  $T_0$  parameter of the Polyakov potentials can induce shifts of the order of several tens of MeV in  $T_c$  (Fig. 1). For  $R = 3$ , we get  $g_1$  of the order of  $6000 \text{ GeV}^{-8}$  and  $T_c = 158\text{--}188$  MeV for the range  $T_0 = 190\text{--}270$  MeV. (ii) Besides the  $8q$  strength, the Polyakov loop plays also a substantial role in decreasing the ratio  $R$ . (iii) The observables calculated at  $\mu = 0$  related with the light quarks, chiral condensates, traced Polyakov loop and dressed Polyakov loop (Fig. 3), chiral and quark number susceptibilities (Fig. 4(a), (d)), as well as the  $s$ -quark number susceptibility (Fig. 4(e)) and Polyakov loop susceptibility (Fig. 4(c)) yield a crossover temperature  $T_t \sim 179$  MeV for  $g_1 = 6000 \text{ GeV}^{-8}$  and  $T_0 = .19$  GeV. (iv) Some of the  $s$ -quark observables show two possible transition temperatures, Fig. 2, 3, 4(b), the first close to the  $u$ -quark transition, the second about 50 MeV higher for the PNJL model. (v) The best fit to the trace anomaly is for  $g_1 = 6000 \text{ GeV}^{-8}$  at  $T_0 = .21$  GeV (Fig. 5(a)) and for the

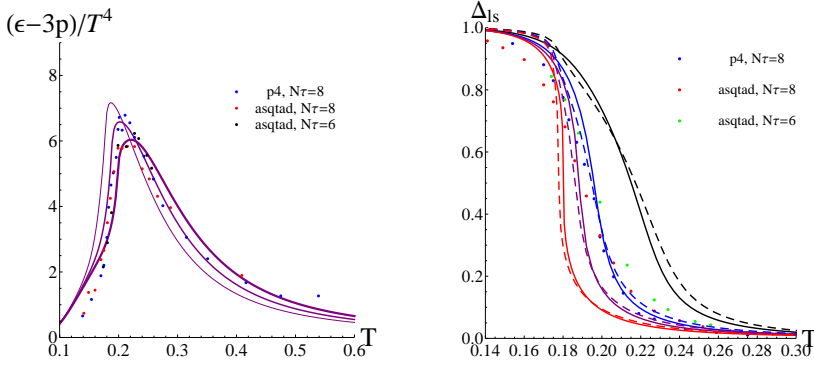


Fig. 5. Left: trace anomaly with  $8q$  strength  $g_1 = 6000 \text{ GeV}^{-8}$ , with  $\mathcal{U}_P$  from [14] and respective parameter  $T_0 = .19, .21, .23 \text{ GeV}$  (which yield peak positions from left to right). The IQCD data is taken from [28]. Right: the IQCD data for  $\Delta_{Is}$ , the subtracted chiral condensate value normalized to its zero  $T$  value, as defined in [28], compared to PNJL calculations for several  $g_1$  strengths, color code as in Fig. 2. Solid lines: with  $\mathcal{U}_P$  from [14], dashed lines: with  $\mathcal{U}_P$  from [15], both at  $T_0 = .19 \text{ GeV}$ .

observable  $\Delta_{Is}$  we obtain a reasonable fit with  $g_1 = 5 \dots 6 \times 10^3 \text{ GeV}^{-8}$  and  $T_0 = .19 \text{ GeV}$  (Fig. 5(b)). (vi) The peak positions and heights of the continuum extrapolated light quark chiral susceptibility vary considerably (Fig. 6). This big spread allows to accommodate a large range of  $g_1$  values, whose peak positions in turn depend also on the choice of the  $T_0$  parameter. The value  $g_1 \sim 5 \times 10^3 \text{ GeV}^{-8}$  is eventually the best choice if one takes the height of the peak also into consideration.

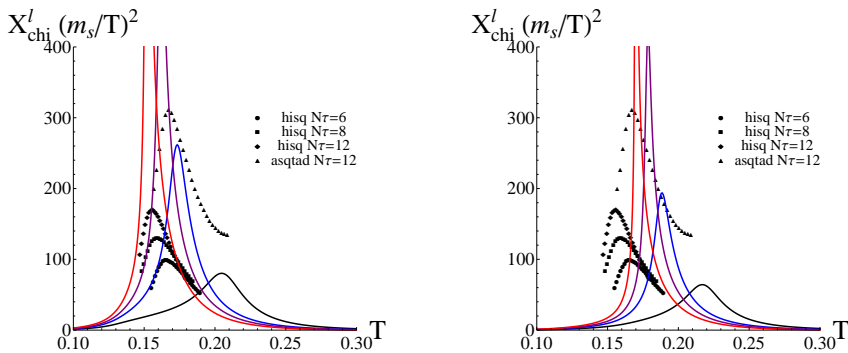


Fig. 6. The IQCD data for the light quark chiral susceptibility  $X_{\text{chi}}^l$  in the continuum limit taken from [2], in comparison with the PNJL model with  $\mathcal{U}_P$  [14] at  $T_0 = .15 \text{ GeV}$  (left panel) and  $T_0 = .19 \text{ GeV}$  (right panel) for different  $g_1$  strengths (solid lines, narrower peaks correspond to increasing  $g_1$ ).

REFERENCES

- [1] J.M. Pawłowski, *AIP Conf. Proc.* **1343**, 75 (2011).
- [2] A. Bazavov *et al.* [HotQCD Collaboration], *Phys. Rev.* **D85**, 054503 (2012).
- [3] S. Borsanyi *et al.*, *Acta Phys. Pol. B Proc. Suppl.* **5**, 1125 (2012), this issue.
- [4] M. Stephanov, *Acta Phys. Pol. B* **35**, 2939 (2004).
- [5] S. Gupta *et al.*, *Science* **332**, 1525 (2011).
- [6] Y. Nambu, G. Jona-Lasinio, *Phys. Rev.* **122**, 345 (1961); **124**, 246 (1961).
- [7] G. 't Hooft, *Phys. Rev.* **D14**, 3432 (1976); **D18**, 2199 (1978).
- [8] V. Bernard, R.L. Jaffe, U.-G. Meissner, *Phys. Lett.* **B198**, 92 (1987).
- [9] H. Reinhardt, R. Alkofer, *Phys. Lett.* **B207**, 482 (1988).
- [10] A.A. Osipov, B. Hiller, J. da Providencia, *Phys. Lett.* **B634**, 48 (2006).
- [11] A.A. Osipov, B. Hiller, A.H. Blin, J. da Providencia, *Ann. Phys.* **322**, 2021 (2007).
- [12] K. Fukushima, *Phys. Lett.* **B591**, 277 (2004).
- [13] E. Megías, E. Ruiz Arriola, L.L. Salcedo, *Phys. Rev.* **D74**, 065005 (2006).
- [14] C. Ratti, M.A. Thaler, W. Weise, *Phys. Rev.* **D73**, 014019 (2006).
- [15] S. Roessner, C. Ratti, W. Weise, *Phys. Rev.* **D75**, 034007 (2007).
- [16] K. Fukushima, *Phys. Rev.* **D77**, 114028 (2008).
- [17] Y. Sakai, K. Kashiwa, H. Kouno, M. Yahiro, *Phys. Rev.* **D77**, 051901 (2008); T. Sasaki, Y. Sakai, H. Kouno, M. Yahiro, *Phys. Rev.* **D82**, 116004 (2010).
- [18] A. Bhattacharyya, P. Deb, S.K. Ghosh, R. Ray, *Phys. Rev.* **D82**, 014021 (2010); A. Bhattacharyya, P. Deb, A. Lahiri, R. Ray, *Phys. Rev.* **D83**, 014011 (2011).
- [19] R. Gatto, M. Ruggieri, *Phys. Rev.* **D83**, 034016 (2011); **D82**, 054027 (2010).
- [20] P. Costa *et al.*, *Phys. Rev.* **D79**, 116003 (2009).
- [21] J. Moreira, B. Hiller, A.A. Osipov, A.H. Blin, *Int. J. Mod. Phys.* **A27**, 1250060 (2012).
- [22] A.A. Osipov *et al.*, *Phys. Lett.* **B646**, 91 (2007).
- [23] A.A. Osipov, B. Hiller, J. Moreira, A.H. Blin, *Phys. Lett.* **B659**, 270 (2008).
- [24] A.A. Osipov, B. Hiller, A.H. Blin, J. da Providencia, *Phys. Lett.* **B650**, 262 (2007).
- [25] B. Hiller, J. Moreira, A.A. Osipov, A.H. Blin, *Phys. Rev.* **D81**, 116005 (2010).
- [26] B.-J. Schaefer, M. Wagner, J. Wambach, *Phys. Rev.* **D81**, 074013 (2010).
- [27] S. Chatterjee, talk at this conference.
- [28] A. Bazavov *et al.*, *Phys. Rev.* **D80**, 014504 (2009).